

Ab initio calculations of structural and electronic properties of CdTe clusters

Somesh Kr. Bhattacharya* and Anjali Kshirsagar^{1†}

Department of Physics, University of Pune, Pune 411 007, India.

(Dated: October 22, 2018)

We present results of a study of small stoichiometric Cd_nTe_n ($1 \leq n \leq 6$) clusters and few medium sized non-stoichiometric Cd_mTe_n [$(m, n = 13, 16, 19)$; ($m \neq n$)] clusters using the Density Functional formalism and projector augmented wave method within the generalized gradient approximation. Structural properties *viz.* geometry, bond length, symmetry and electronic properties like HOMO-LUMO gap, binding energy, ionization potential and nature of bonding *etc.* have been analyzed. Medium sized non-stoichiometric clusters were considered as fragments of the bulk with T_d symmetry. It was observed that upon relaxation, the symmetry changes for the Cd-rich clusters whereas the Te-rich clusters retain their symmetry. The Cd-rich clusters develop a HOMO-LUMO gap due to relaxation whereas there is no change in the HOMO-LUMO gap of the Te-rich clusters. Thus, the symmetry of a cluster seems to be an important factor in determining the HOMO-LUMO gap.

PACS numbers: 61.46.-w, 61.46.Df, 71.15.Mb, 73.22.-f

I. INTRODUCTION

Semiconductor nanoparticles or Quantum Dots (QDs), in particular of II-VI materials, have received tremendous attention during the last two decades owing to their unusual physical properties and wide range of applications¹. A systematic study of QDs is useful to understand the evolution of their physical and chemical properties with size. Moving from a molecule to bulk, one can observe a range of variation of fundamental properties. This size dependent effect, however, is most significant for small sized clusters and is attributed to the different geometry of clusters in comparison to the bulk. Quantum confinement of electronic states and large surface to volume ratio modify the properties of these clusters. In bare clusters, unsaturated bonds lead to peculiar structural and electronic properties like surface reconstruction, formation of new cleavage planes *etc.*

The differences in the structural properties also affect the electronic properties of the QDs. In bulk systems one observes quasi-continuous electronic levels forming bands whereas in clusters the electronic levels are discrete. Apart from the structural and electronic properties, other properties like the thermodynamic and optical properties too differ significantly for clusters as compared to bulk^{2,3}.

Among the II - VI semiconductors, CdX ($X = S, Se, Te$) have potential application in optical and optoelectronic devices. CdTe nanoclusters, in particular, are used in optical sensors. Multilayered CdTe with poly (diallyl dimethyl ammonium chloride) are electro and photoactive and hence are used in neuroprosthetic devices⁴. Self assembled CdTe nanodots have high efficiency in terms of photoluminescence and hence are very good for the purpose of making LEDs. CdTe and Au nanohybrid materials have photoluminescence variation depending upon environmental condition like temperature, ionic strength, solvents and hence are used as biosensors⁵.

We present Density Functional Theory (DFT) based

calculations for some small, Cd_nTe_n ($1 \leq n \leq 6$), and few medium sized Cd_mTe_n ($m, n = 13, 16, 19$) ($m \neq n$) clusters. Both Cd and Te in bulk phase exist in hexagonal structure with c/a ratio 1.89 and 1.33 respectively⁶ whereas CdTe in bulk phase has lattice constant $a = 6.48 \text{ \AA}$ in zincblende structure and $a = 4.57 \text{ \AA}$ and $c = 7.47 \text{ \AA}$ in wurtzite structure. CdTe has a calculated direct band gap of 1.59eV at the Γ point⁷.

Study of small clusters is challenging due to lack of experimental structural information and increased degree of freedom. Very small clusters (containing up to 8-10 atoms) exhibit symmetry and have only a few possible geometries. On the other hand, medium-sized clusters can be considered as fragments of bulk possessing the same structural symmetry as that of the bulk⁸. To the best of our knowledge, so far no *ab-initio* calculations have been reported on CdTe QDs. We compare our results for small CdTe QDs with those of CdS and CdSe wherever available.

Structural, electronic and optical properties of II-VI semiconductor nanoclusters have been studied using a variety of methods based on *ab-initio* DFT, quantum chemistry methods like Hartree-Fock, Gaussian *etc.* and approximate methods like tight-binding method⁹⁻¹².

II. METHODOLOGY AND COMPUTATIONAL DETAILS

The first step for calculating the cluster properties is the determination of the lowest energy configuration. Existence of several configurations with varying coordination and multiple minima in the potential energy surface enormously complicate the problem making it almost impossible to decide by direct calculation of the lowest energy configuration for clusters.

In this work we have used Born-Oppenheimer molecular dynamics within the Kohn-Sham density functional framework¹³. The electronic structure is calculated

self-consistently using projector augmented wave (PAW) method¹⁴ as implemented in VASP package¹⁵ within the framework of GGA instead of *Vanderbilt* ultra-soft pseudo-potential(US-PP)¹⁶ as it provides better first principle simulations as compared to US-PP¹⁴. In pseudo potential methods, the effect of core electrons and nuclei is replaced by an effective ionic potential and only the valence electrons which are directly involved in chemical bonding are considered.

Various parameterizations have been used for different exchange-correlation potentials¹⁷ in the DFT formalism in the literature. It has been reported that generalized gradient approximation (GGA) gives much better results for binding energy and band gap as compared to local density approximation (LDA) and therefore we have used GGA, as developed by Perdew-Berke-Ernzerhof (PBE)¹⁸ for our calculation. PBE is known to improve total energy and molecule atomization energy and therefore the electronic properties, as compared to PW91¹⁹ and the results agree with that of the experiments very well.

The geometry of small clusters varies significantly from that of the bulk. We have chosen several possible initial geometries by exploiting the symmetry considerations and by exchanging the positions of anionic and cationic atoms. The number of initial structures is small for very small clusters. But for clusters with 10-12 atoms, lot many configurations have been used to determine the lowest energy structure.

For structure optimization we have used a super-cell of size $a = 25\text{\AA}$ and the plane wave cut-off was set to be 274.3 eV. These values are chosen after performing calculations for different cell sizes and cutoff energies. We have employed conjugate gradient (CG) technique implemented via Kosugi algorithm²⁰ (special Davison block iteration scheme) for optimizing geometry.

The valence electron configurations used for Cd and Te are $5s^24d^{10}$ and $5s^25p^4$ respectively. The $4d$ levels in Te atom are well separated from the $5s$ level and hence can be included in the core.

CdTe in bulk has zincblende (ZB) structure with T_d symmetry. Therefore for medium sized non-stoichiometric clusters Cd_mTe_n ($m \neq n$), the initial geometry was considered as a fragment of the ZB structure. The size of the super-cell was chosen to be $a = 30\text{\AA}$ which is sufficiently large to minimize inter-cluster interactions even for the largest cluster size we consider in this work. In all the structure minimizations, the force and energy convergence obtained was $\sim 10^{-3}$ eV/ \AA and $\sim 10^{-4}$ eV respectively.

III. RESULTS AND DISCUSSIONS

A. Structural properties of Cd_nTe_n

The geometries for lowest energy (LE) of Cd_nTe_n obtained by CG are shown in Fig. 1 and the first local minima (FLM) in Fig. 2. It is interesting to note that for all

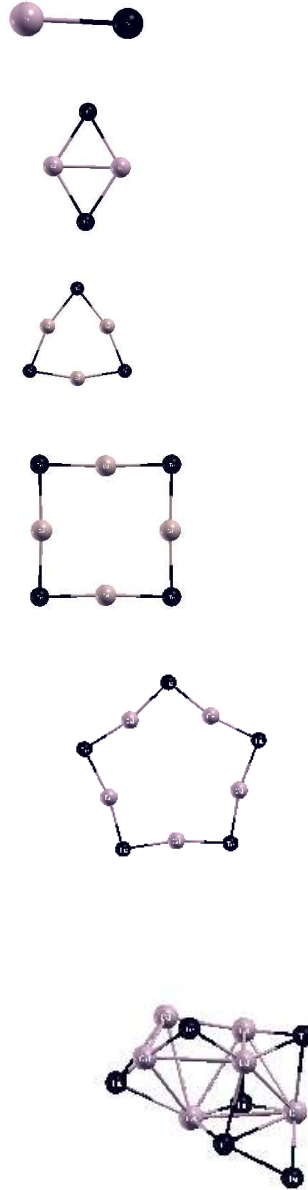


FIG. 1: Lowest energy configuration of Cd_nTe_n for ($1 \leq n \leq 6$) The grey atoms are Cd and the black atoms are Te.

the calculated lowest energy structures, the chalcogenide atoms are at the peripheral positions. This is a direct consequence of Coulomb repulsion between the lone-pairs situated on the chalcogenide atoms which is minimized by separating the chalcogenide atoms towards the peripheral position. As expected, the ground state structures of these CdTe clusters do not resemble the bulk phase.

CdTe dimer is a linear molecule with bond length of 2.57\AA and belongs to $C_{\infty v}$ point group. For Cd_2Te_2 , Cd_3Te_3 , Cd_4Te_4 , Cd_5Te_5 and Cd_6Te_6 , there are two possible lowest energy configurations within the energy difference of $\sim 0.11\text{eV}$, $\sim 0.22\text{eV}$ $\sim 0.04\text{eV}$, $\sim 0.05\text{eV}$ and

$\sim 0.09\text{eV}$ per atom, respectively. Except for Cd_6Te_6 , the lowest energy geometry is a planar ring-like structure. Cd_2Te_2 has LE as the rhombic structure and a square planar structure as FLM. The LE and FLM belong to D_{2h} and C_{2v} point group respectively. Cd_3Te_3 has triangular structure (D_{3h} point group) as LE configuration and another planar structure (C_s point group) as the FLM. No three dimensional (3D) stable geometry is obtained for $n = 2, 3$. For Cd_4Te_4 , the square planar (D_{4h} point group) geometry is obtained for LE and 3D tetrahedral structure (T_d point group) as FLM. Cd_5Te_5 is a planar pentagon (C_s point group) in LE and a non-symmetric 3D structure as FLM. A transition from planar LE to 3D LE occurs for $n = 6$. This is attributed, as explained later, to the tendency of achieving higher coordination without putting too much strain on the bond angles. All the atoms in planar clusters, except for the FLM of Cd_3Te_3 , have coordination 2.

The geometries obtained for the CdTe clusters are quite similar to those of corresponding CdS and CdSe clusters upto $n = 4$ ²¹. However, the geometries of Cd_5Te_5 and Cd_6Te_6 are very different from the CdS and CdSe counterparts²¹. This difference may be attributed to the fact that we have included 4d of Cd in the valence configuration in the present study. The necessity of including 4d electrons of the cations in the valence configuration has been emphasized by Wei and Zunger²².

As we move from planar to 3D structure the coordination of atoms increases from 2 to 3 and in some cases 4. The 3D structures of Cd_4Te_4 , Cd_5Te_5 and Cd_6Te_6 can be considered to be made up of smaller cluster units namely Cd_2Te_2 and Cd_3Te_3 .

A comparison of Cd_nTe_n clusters with Cd_n ²³ shows that three dimensional structures are more favorable in pure Cd clusters as compared to CdTe clusters where planar structure is favored even for 10 atom cluster.

Figure 3 shows the variation of average Cd-Te bond length with the number of atoms in the clusters. The near neighbour (nn) distance for CdTe bulk is 2.81\AA . As evident from Fig. 3, these clusters have an average bond length less than the nn distance in bulk. This is due to incomplete coordination in these clusters on account of very small number of atoms. The bond length of CdTe dimer is the smallest. In fact, the smallest Cd-Te bond length remains almost constant in these clusters for $n = 3 - 6$ (not shown in figure). The average Cd-Te bond length shrinks with increasing n in planar structures ($n = 2 - 5$) and increases in going from planar to 3D structures.

Surface studies²⁴ on heteropolar covalent and ionic semiconductors have identified quantum mechanical electron-electron Coulomb repulsion, hybridization effects and classical Coulomb attraction between anion and cation as competing factors in deciding the stability of the surface. The last factor seems to be more important with only 3 neighbours for atoms on the surface. Optimum energy gain is achieved when the distance between anion and cation is as small as possible. Thus shorter bonds are more ionic in nature. We therefore expect that

CdTe dimer will have more ionic character as compared to other clusters. In Cd_2Te_2 , there exist a covalent bond between Cd-Cd which accounts for an increase in average Cd-Te bond length. As explained later from the charge density plots, there are no covalent bonds between either Cd-Cd or Te-Te in other planar structures ($n = 3 - 5$). Therefore, the average Cd-Te bond length is smaller in these clusters. In Cd_6Te_6 , bonds between similar atoms appear and as a result the average Cd-Te bond length increases.

Cd-Cd bond length in Cd_2Te_2 is smaller (2.87\AA) than in Cd dimer (3.47\AA). The average Cd-Cd bond length is same in Cd_3Te_3 and Cd_3 . However, it is larger in Cd_nTe_n as compared to Cd_n for $3 \leq n \leq 6$. In contrast, average Te-Te bond length is significantly larger in CdTe clusters in comparison to pure Te clusters as expected due to lone pair repulsion. Also it does not appreciably change with n .

Average Te-Cd-Te bond angle increases from 107.2° in Cd_2Te_2 to nearly 180° in Cd_4Te_4 . The angle further opens up in Cd_5Te_5 . In Cd_6Te_6 , all the Te-Cd-Te angles are smaller than linear angle as a consequence of 3D structure. Thus we see that smaller clusters have a tendency to form linear Te-Cd-Te bonds resulting in planar structures with coordination of 2 and as higher coordination number takes over, a transition from planar to three dimensional structure results for stable geometry.

All the clusters are found to be stable against fragmentation into smaller clusters.

B. Electronic properties of Cd_nTe_n

Figures 4 and 5 show the variation in the highest occupied molecular orbital (HOMO) - lowest unoccupied molecular orbital (LUMO) gap (E_g) and binding energy (defined in Eq. (1) per Cd-Te unit with the number of Cd-Te units in the cluster.

$$E_b = [n\{E(\text{Cd}) + E(\text{Te})\} - E(\text{Cd}_n\text{Te}_n)]/n \quad (1)$$

The corresponding two curves for CdS and CdSe show similar trends²¹ and the authors claim to infer the stability of clusters from the maximum in these curves. However, we do not see any such correlation for the clusters studied in the present work. It is seen that Cd_5Te_5 is more stable compared to its neighbours. It may be mentioned that the number of electrons in this system are 90 which matches with the shell closing number for jellium-like systems.

We have calculated the vertical detachment energy (VDE), shown in Fig. 6, and the electron affinity (EA), shown in Fig. 7, using Eqs. (2) and (3) by performing two self-consistent calculations for different electronic systems without allowing any change in the lowest energy geometry of the neutral cluster.

$$VDE(\text{Cd}_n\text{Te}_n) = E(\text{Cd}_n\text{Te}_n^+) - E(\text{Cd}_n\text{Te}_n) \quad (2)$$

$$EA(Cd_nTe_n) = E(Cd_nTe_n^-) - E(Cd_nTe_n) \quad (3)$$

In bulk CdTe, the bonding is largely covalent as the atomic number and hence the atomic radii for Cd and Te are very close. As a result, the Coulombic forces between the two species are balanced very well. However due to difference in electronegativity of Cd and Te, the bonding has some ionic character even in the bulk.

We show total charge density iso-surface plots for CdTe dimer and Cd₂Te₂ cluster in Figs. 8 and 9 respectively, revealing covalent bonding. Similar charge density distributions are seen for other clusters too. No Cd-Cd or Te-Te near neighbour bonds are seen to be formed for clusters with $n > 2$. The charge density plots for CdS and CdSe²¹ show that the bonding has some ionic character and is not purely covalent. Ionicity in bonding is more in CdS than in CdSe because of smaller atomic radius of sulphur. Ionicity is expected to be still smaller in CdTe.

An analysis of charge inside atomic spheres with covalent radii shows that the distribution of charge in the Cd and Te spheres is almost same for planar structures for $n = 3 - 5$. There is more charge localization in planar structures in comparison to CdTe dimer, Cd₂Te₂ and the 3D structures.

A more detailed information regarding the bonding in these clusters can be obtained from the partial charge density plots of the molecular orbitals (MOs) in these clusters.

From Figs. 10 and 11 it is evident that the HOMO consists of purely Te p and in the LUMO Cd s and p hybridize to give a sp -hybrid orbital which in turn forms a σ bond with the Te p orbital. Similar trends are seen for the plots for HOMO and LUMO of Cd₃Te₃ as shown in Figs. 12 and 13. Figure 13 also shows the delocalization of the charge density in the central region of the clusters indicating a semi-metallic character in the bonding. Thus, these systems will favour electron addition as is also evident from Fig. 7. For other clusters the partial charge density for HOMO and LUMO have similar nature.

As seen from the MO charge distribution of HOMO as one goes from $n = 2$ to $n = 6$, an enhancement in delocalisation results accounting for a steady decrease in the VDE as shown in Fig. 6.

In Fig. 14 we show the one-electron energies for all the CdTe clusters and the atomic levels of Cd and Te. The Cd s and the Te p levels lie in the same energy window in the atomic case. Consequently, an intermixing of these orbitals occurs in the clusters. A fat band analysis of the CdTe bulk band structure (not shown here) using full potential linear augmented plane wave method²⁵ reveals similar intermixing of orbitals. Thus, the bulk type hybridization of the orbitals is retained in clusters. The movement of the the HOMO and LUMO in these small clusters is quite interesting. As the cluster size increases, the HOMO moves downward whereas

the LUMO moves upward resulting in widening of the HOMO-LUMO gap. However, this shift is not uniform. The HOMO moves downward slowly as compared to the LUMO which moves upward rapidly. But for Cd₆Te₆, the HOMO shifts slightly upward and the LUMO shifts downward resulting in a smaller HOMO-LUMO gap as a consequence of planar to 3D transition in geometry.

C. Properties of Cd_mTe_n clusters

CdTe, with many other II-VI semiconductors, in bulk has ZB and wurtzite (W) phases possible. There are also reports of size induced phase transitions in ZnS²⁶ and CdS²⁷ nanoparticles. The first coordination for central atom is identical in ZB and W phases. If we consider the trigonal axis [111] in ZB and [001] in W then three near neighbours are identical.

We have, therefore, performed calculations for four larger non-stoichiometric CdTe clusters *viz.* Cd₁₃Te₁₆ (central atom + 3 neighbouring shells), Cd₁₆Te₁₉ (central atom + 4 shells), Cd₁₆Te₁₃ and Cd₁₉Te₁₆. The later two geometries are obtained from the former two by interchanging the positions of Cd and Te atoms. These clusters have been considered as fragments of the bulk and hence their initial symmetry is T_d as shown in Figs. 15(a) and 16(a).

Cd₁₃Te₁₆ has a central Cd atom and the side view of its relaxed structure is shown in Fig. 15(b). Figure 15(c) shows the side view of relaxed structure of Cd₁₆Te₁₃ which has a central Te atom. During relaxation the central Te atom pushes the neighboring Cd atoms outward. Figure 16 shows the top views of initial geometry for Cd₁₆Te₁₉(a) and the relaxed geometries for Cd₁₆Te₁₉(b) and Cd₁₉Te₁₆(c). It is found that upon relaxation only the Te-rich clusters retain their T_d symmetry whereas the Cd-rich clusters attain lower symmetry structures.

We summarize in table I some of the structural and electronic properties of Cd_mTe_n clusters. It may be mentioned that the binding energy of CdTe dimer is 0.76 eV/atom whereas the cohesive energy of CdTe bulk is 4.9 eV.

TABLE I: Summary of Structural and Electronic properties of relaxed Cd_mTe_n ($m \neq n$) clusters. PG is the observed point group symmetry, BE is binding energy expressed in (eV/atom), l is average Cd-Te bond length in Å, θ is the Y-X-Y bond angle at the central atom X of the cluster and E_g is the HOMO-LUMO gap in eV.

| Clusters | PG | BE | l | θ | E _g |
|-----------------------------------|-----------------|------|------|----------|----------------|
| Cd ₁₃ Te ₁₆ | T _d | 2.13 | 2.81 | 109.47° | 0.195 |
| Cd ₁₆ Te ₁₃ | C _{3v} | 1.95 | 2.84 | 109.48° | 0.659 |
| Cd ₁₆ Te ₁₉ | T _d | 2.14 | 2.82 | 109.47° | 0.088 |
| Cd ₁₉ Te ₁₆ | C ₁ | 1.95 | 2.81 | 91.31° | 0.964 |

A comparison of the binding energies of the above clus-

ters indicates that $\text{Cd}_{13}\text{Te}_{16}$ and $\text{Cd}_{16}\text{Te}_{19}$ are more stable than $\text{Cd}_{16}\text{Te}_{13}$ and $\text{Cd}_{19}\text{Te}_{16}$. In the former group the Te atoms are on the surface and hence these structures are energetically favoured as discussed earlier for smaller clusters. For the Te-rich clusters, the relaxation is not strong enough to break their initial T_d symmetry. On the other hand, the Cd-rich clusters, being weakly bound, go to lower symmetry structures upon relaxation. A comparison of binding energy per atom for Cd_mTe_n with corresponding Hg_mTe_n clusters⁸ shows an increase. This is attributed to symmetry allowed pd interactions. The d levels of Hg are closer than those of Cd to the p levels of Te. Therefore pd -repulsion induced bond weakening is more in HgTe than in CdTe clusters resulting in a reduction of binding energy.

A very interesting feature observed in the Cd-rich clusters is Jahn-Teller distortion. The initial HOMO-LUMO gap for $\text{Cd}_{16}\text{Te}_{13}$ and $\text{Cd}_{19}\text{Te}_{16}$ is nearly zero. But upon relaxation, they attain an appreciable HOMO-LUMO gap. This is a clear indication that the energy levels which are nearly degenerate in the initial structure have moved apart during relaxation. Thus, relaxation has destroyed symmetry resulting in the lifting of degeneracy. On the other hand for the Te-rich clusters, the HOMO-LUMO are not degenerate (though close to each other) and thus there is no Jahn-Teller distortion. Similar trend has also been observed in non-stoichiometric HgTe clusters⁸. The Hg-rich clusters upon relaxation lose their initial T_d symmetry. As a result, they attain a definite bandgap and a semi-metal to semiconductor transition is observed. Dalpian *et al.* have shown that symmetry is an important parameter in deciding the properties of nanoclusters²⁸.

IV. CONCLUSION

The ground state geometries of Cd_nTe_n ($1 \leq n \leq 6$) were calculated using *ab-initio* DFT. The structures do not

resemble that of the bulk phase. The Cd atoms tend to form a core group surrounded by the chalcogenide atoms because of the Coulomb repulsion of the lone pair of p -electrons on Te. For Cd_nTe_n , ($1 \leq n \leq 5$), the planar geometry is the lowest energy configuration as Te-Cd-Te prefer to form linear bond. But as the number of atoms increases further, higher coordination takes over and three dimensional structures result. Bonding in CdTe clusters is mostly covalent in nature with partial ionic character. The degree of ionicity changes with n . Hybridization of orbitals in these clusters is observed to be same as that in the bulk.

The relaxed structures of non-stoichiometric clusters, Cd_mTe_n with ($m, n = 13, 16, 19$ and $m \neq n$), were obtained using *ab-initio* DFT with the wavefunction projected to real space. The Te-rich clusters with Te atoms on the surface, are found to be more stable than the Cd-rich clusters. The symmetry of the cluster plays a vital role in determining its HOMO-LUMO gap. It was found that the Cd-rich cluster lose their initial T_d symmetry and attain a large HOMO-LUMO gap as compared to the Te-rich clusters.

V. ACKNOWLEDGMENT

We acknowledge financial support from the Department of Science & Technology, Government of India. We also thank IUCAA, Pune and Centre for Modeling and Simulation, University of Pune for use of their computational facilities.

* Electronic address: skb@physics.unipune.ernet.in

† Electronic address: anjali@physics.unipune.ernet.in

¹ Corresponding author.

¹ V. L. Colvin, M. C. Schlamp and A. P. Alivisatos, *Nature* (London) **370**, 354 (1994); A. P. Alivisatos, *J. Phys. Chem.* **100**, 13226 (1996).

² S. Ögöt, J. R. Chelikowsky, S. G. Louie, *Phys. Rev. Lett.* **79** 1770 (1997); I. Vasiliev, S. Ögöt and J. R. Chelikowsky, *Phys. Rev. B* **65**, 115416 (2002) and references therein.

³ A. Shvartsberg (private communication).

⁴ M. Gao, C. Lesser, S. Kirstein, H. M^ohwald, A.L. Rogach and H. Weller, *J. Appl. Phys.* **87**, 2297 (2000).

⁵ Li J *et al.*, *Chem. Commn. (Camb.)* **8**, 982 (2004).

⁶ N. W. Ashcroft and N. David Mermin, *Solid State Physics*, (Holt-Saunders, Philadelphia, 1981).

⁷ M. L. Cohen and J. R. Chelikowsky in *Electronic Structure and Optical Properties of Semiconductors* edited by

M. Cardona, (Springer-Verlag, Berlin, 1988).

⁸ X. Q. Wang, S. J. Clark and R. A. Abram, *Phys. Rev. B* **70**, 235328 (2004).

⁹ V. S. Gurin, *Int. J. Q. Chem.* **71**, 337 (1999); J. -O. Joswig *et al.*, *J. Phys. Chem. B* **104**, 2617 (2000); A. J. Williamson and A. Zunger, *Phys. Rev. B* **61**, 1978 (2000); J. M. Matxain, J. E. Fowler and J. M. Ugalde, *Phys. Rev. A* **61**, 053201 (2000); J. M. Matxain, J. M. Mercero, J. E. Fowler and J. M. Ugalde, *Phys. Rev. A* **64**, 053201 (2001).

¹⁰ J. Muilu and T. A. Pakkanen, *Sur. Sci.* **364**, 439 (1996).

¹¹ E. Spano, S. Hamad and C. R. Catlow, *J. Phys. Chem.* **13**, 10337 (2003).

¹² V. Albe, C. Jouanin and D. Bertho, *J. Crys. Gr.* **184/185**, 388 (1998); S. Pokrant and K. B. Whaley, *Eur. Phys. J. D* **6**, 255 (1999).

¹³ P. Hohenberg and W. Kohn, *Phys. Rev.* **136**, B864 (1964); W. Kohn and L. J. Sham, *Phys. Rev.* **140**, A1133 (1965).

- ¹⁴ P. E. Blöchl, Phys. Rev. B **50**, 17953 (1994); G. Kresse and J. Joubert, Phys. Rev. B **59**, 1759 (1999).
- ¹⁵ G. Kresse and J. Furthmüller, Phys. Rev. B **54**, 11169 (1996); Comput. Mater. Sci. **6**, 15 (1996).
- ¹⁶ A. Pasquarello, K. Laasonen, R. Car, C. Lee and D. Vanderbilt, Phys. Rev. Lett. **69** 1982 (1992); K. Laasonen, A. Pasquarello, R. Car, C. Lee and D. Vanderbilt, Phys. Rev. B **47**, 10142 (1993).
- ¹⁷ O. Gunnarsson and R. Jones in *Local Density Approximations in Quantum Chemistry and Solid State Theory*, edited by J.P. Dahl and J. Avery, (Plenum, New York, 1983), pp. 229.
- ¹⁸ J. P. Perdew, K. Burke and M. Ernzerhof, Phys. Rev. Lett. **77**, 3865 (1996).
- ¹⁹ J. P. Perdew *Electronic Structure of Solids '91*, edited by P. Ziesche and H. Eschrig (Akademie Verlag, Berlin, 1991), pp. 11; J.P. Perdew and Y. Wang, Phys. Rev. B **45**, 13244 (1992).
- ²⁰ N. Kosugi, J. Comput. Phys. **55**, 426 (1984).
- ²¹ M. C. Tropicovsky and J. R. Chelikowsky, J. Chem. Phys. **114**, 943 (2001).
- ²² S. -H. Wei and A. Zunger, Phys. Rev. B **37**, 8958 (1988); J. Cry. Gr. **86**, 1 (1988).
- ²³ J. Zhao, Phys. Rev. A **64**, 043204 (2001).
- ²⁴ D. Vogel, P. Krüger and J. Pollmann, Sur. Sci. **402-404**, 774 (1998).
- ²⁵ P. Blaha, K. Schwarz, P. Sorantin and S.B. Trickey, Comp. Phys. Commun. **59**, 399 (1990).
- ²⁶ J. Nanda and D. D. Sarma, J. Appl. Phys. **90**, 2504 (2001).
- ²⁷ T. Nanba, Y. Nodake, M. Muneyasu, G. P. Williams and S. Hayashi, J. Phys. Soc. Jpn. **66**, 1526 (1997); R. Banerjee, R. Jayakrishnan and P. Ayyub, J. Phys. : Cond. Matt. **12**, 10647 (2000).
- ²⁸ G. M. Dalpian, M. L. Tiago, M. L. Puerto and J. R. Chelikowsky, Nano Lett. **6**, 501 (2006).

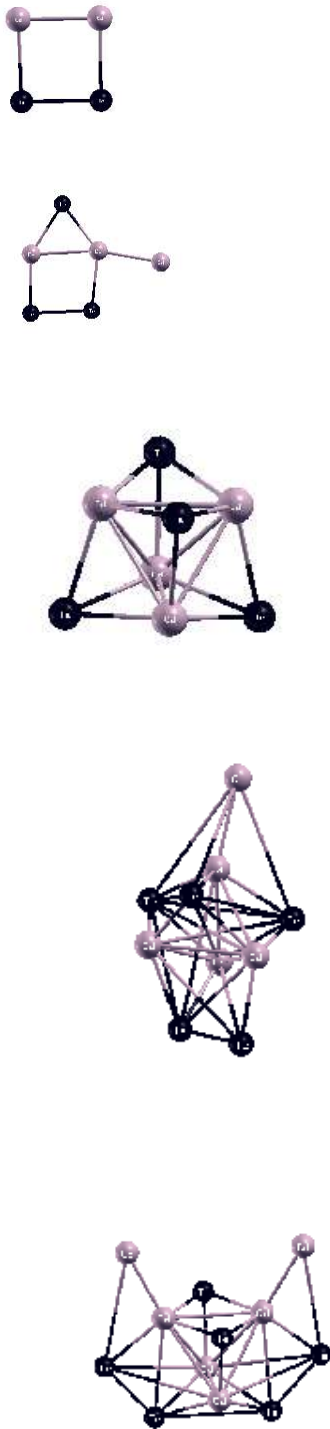


FIG. 2: Geometries of the first local minima of Cd_nTe_n for $(1 \leq n \leq 6)$.

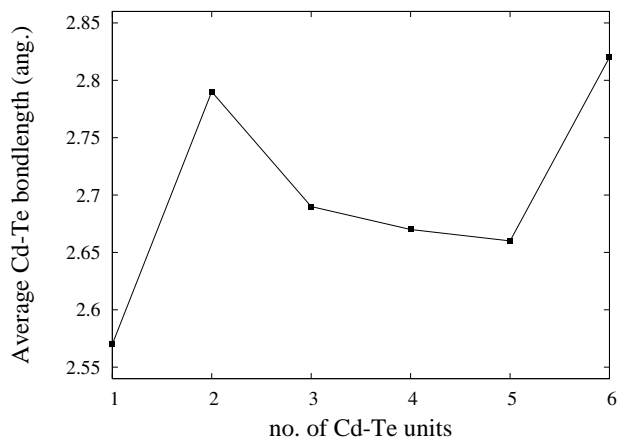


FIG. 3: Average Cd-Te bond length in Å *vs* number of Cd-Te units.

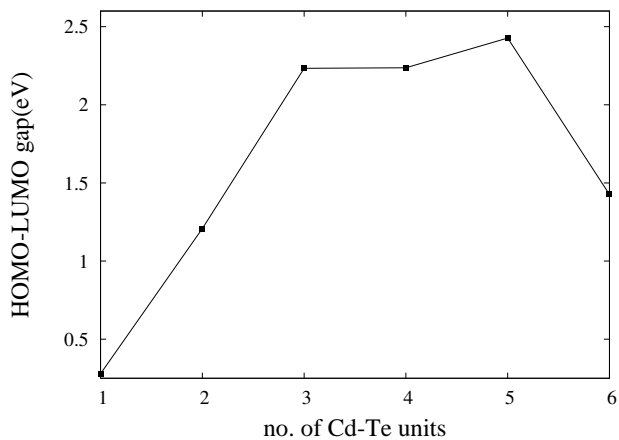


FIG. 4: HOMO-LUMO gap in eV *vs* number of Cd-Te units.

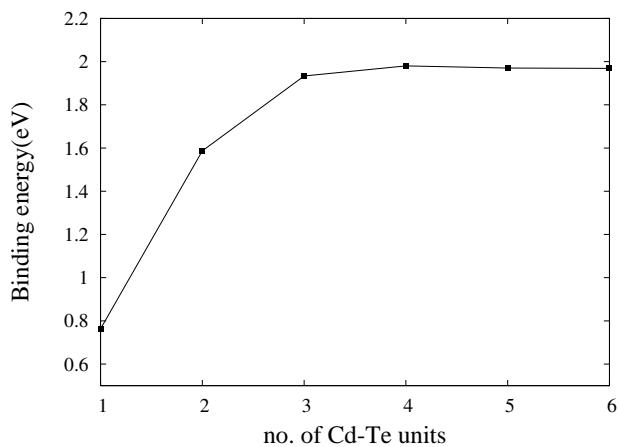


FIG. 5: Binding energy in eV *vs* number of Cd-Te units.

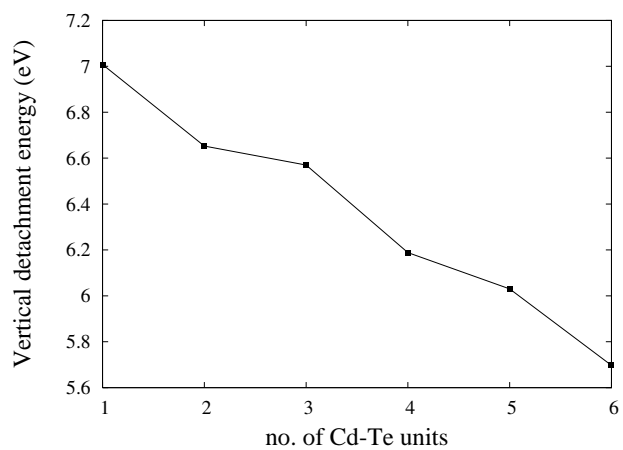


FIG. 6: Vertical detachment energy (eV) *vs* number of Cd-Te units.

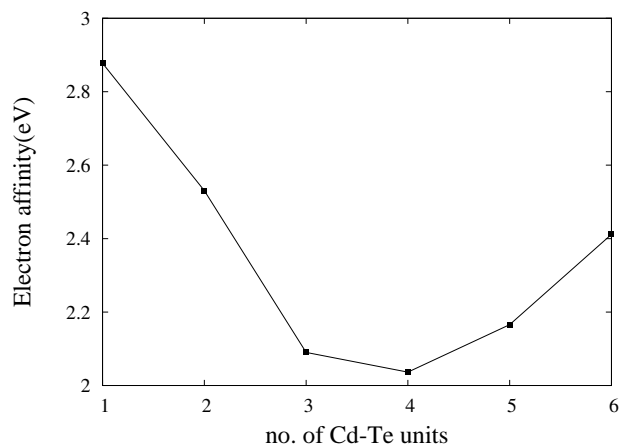


FIG. 7: Electron affinity in eV *vs* number of Cd-Te units.

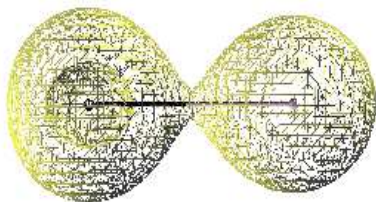


FIG. 8: Charge density iso-surface for CdTe dimer.



FIG. 9: Charge density iso-surface for Cd₂Te₂. The grey atoms are Cd and black atoms are Te.

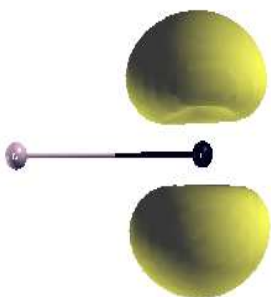


FIG. 10: Iso-surface of partial charge density of HOMO for CdTe dimer.

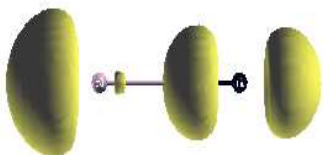


FIG. 11: Iso-surface of partial charge density of LUMO for CdTe dimer.

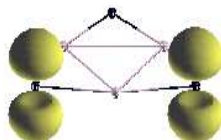


FIG. 12: Iso-surface of partial charge density of HOMO for Cd₃Te₃.

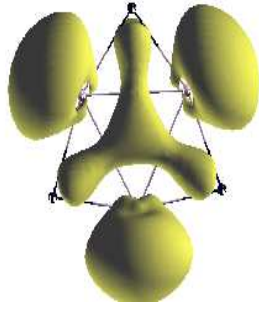


FIG. 13: Iso-surface of partial charge density of LUMO for Cd_3Te_3 .

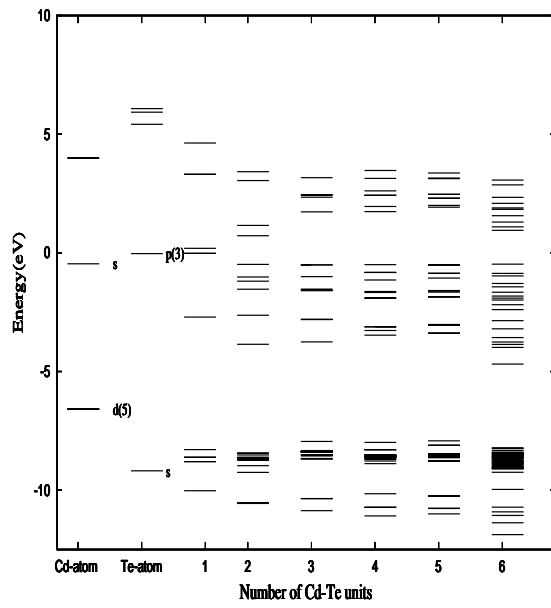
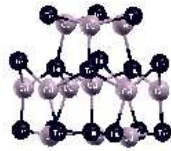


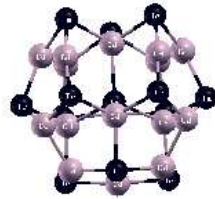
FIG. 14: Energy level diagram of CdTe clusters.



(a) $Cd_{13}Te_{16}$: initial



(b) $Cd_{13}Te_{16}$: relaxed



(c) $Cd_{16}Te_{13}$: relaxed

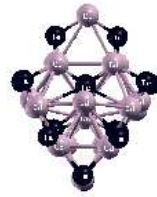
FIG. 15: Side view of the initial and relaxed geometries.



(a) $Cd_{16}Te_{19}$: initial



(b) $Cd_{16}Te_{19}$: relaxed



(c) $Cd_{19}Te_{16}$: relaxed

FIG. 16: Top view of the initial and relaxed geometries.